ELSEVIER

Sensors and Actuators A 50 (1995) 81–86

SENSORS AND ACTUATORS A PHYSICAL

A bidirectional silicon micropump

R. Zengerle [a,*], J. Ulrich [b], S. Kluge [c], M. Richter [c], A Richter [c]

[a] *Hahn-Schickard-Gesellschaft, Institut für Mikro und Informationstechnik, Wilhelm-Schickard-Straße 10, D-78052 Villingen-Schwenningen, Germany*
[b] *Siemens AG, ZPL1 MPP4, Otto-Hahn-Ring 6, D-81739 Munich, Germany*
[c] *Fraunhofer Institut für Festkörpertechnologie, Hansastraße 27d, D-80686 Munich, Germany*

Received 1 May 1995; in revised form 6 September 1995; accepted 21 September 1995

Abstract

In this paper we present a bidirectional silicon micropump. It consists of an electrostatically actuated diaphragm and two passive check valves. It differs from other well-known diaphragm pumps, generally referred to as unidirectional pumps, in the layout of the valves. We have designed a flap valve with a first mechanical resonance frequency between 1 and 2 kHz (in the fluid environment). At low actuation frequencies (0.1–800 Hz), the pump works in the forward mode. At higher frequencies (2–6 kHz) the pump operates in the reverse direction. This is due to a phase shift between the response of the valves and the pressure difference that drives the fluid. Investigating different pump layouts, we achieve maximum pump rates of 250 and 850 μl min^{-1} in the forward direction as well as 400 and 200 μl min^{-1} in the reverse direction. The maximum back pressure is 31 000 Pa (3.1 m H_2O) in the forward and 7000 Pa (0.7 m H_2O) in the reverse direction.

Keywords: Pumps; Actuators; Electrostatic drive; Micropumps; Microactuators; Micromachining

1. Introduction

At the moment many efforts are directed to the development of miniaturized chemical analysis systems in order to get portable and stand-alone on-line analysers. Several micromachined pumps have been developed for fluid handling in these systems [1] and most of the pumps are of the reciprocating type [2–8]. They consist of a displacement unit and two passive check valves (Fig. 1) or diffuser/nozzle elements.

In the case of an electrostatically driven displacement unit [4], the pump is normally actuated by a square wave with an amplitude of 150–200 V and frequencies of 0.1 Hz up to several hundred hertz. When the supply voltage is applied between the pump diaphragm and the counter electrode, the diaphragm is driven by electrostatic forces and bends towards the counter electrode. Thereby fluid will be sucked in through the inlet valve. When the supply voltage is turned off, the diaphragm springs back, forcing fluid out through the outlet valve. Two passive check valves direct the flow from inlet to outlet. Therefore miniaturized diaphragm pumps are known as unidirectional pumps. The outer dimensions of the electrostatically actuated diaphragm pump are 7 mm×7 mm×2 mm. We achieved maximum pump rates of 850 μl min^{-1}

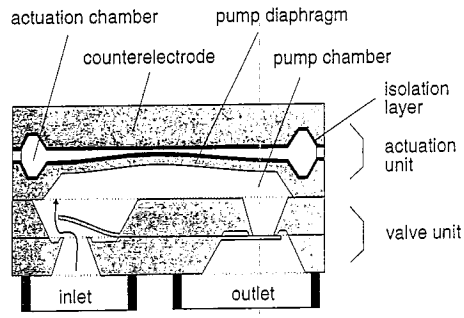

Fig. 1. Schematic view of an electrostatically driven diaphragm pump [4].

and a maximum hydrostatic back pressure of 31 000 Pa (3.1 m H_2O) at a supply voltage of 200 V. The total power consumption of the pump element is less than 1–5 mW in this operation mode and the strong electrostatic field is separated completely from the fluid.

There are two practical limitations for fluid handling using micromachined pumps in chemical analysis systems: (i) the leakage of the microvalves, if unfiltered solutions are used; (ii) the dead volume of the pump chamber. It is possible to overcome these limitations by an experimental set-up depicted in Fig. 2 [9]. A wash pump is used in order to purge the system with a filtered wash solution. A sample pump is used in order to suck in the sample fluid just up to a fluid level between the reference electrode and the detector electrode. So micropumps are not in contact with the unknown

* Corresponding author. Fax: +49-7721-943234. E-mail: zengerle@imit.uni-stuttgart.de.

SSDI 0924-4247(95)01058-1

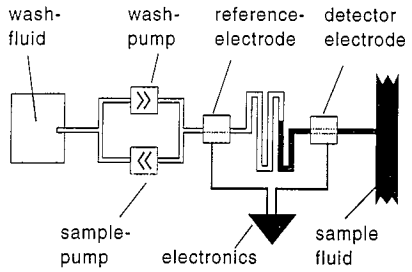

Fig. 2. Set-up of an integrated analysis system [9].

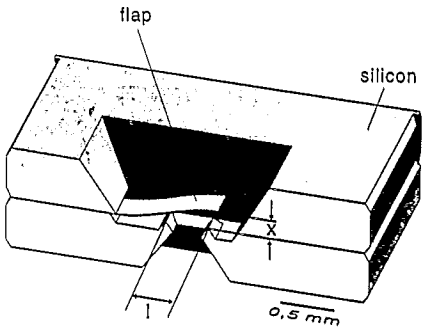

Fig. 3. Miniaturized flap valve (length, 1700 μm; width, 1000 μm; thickness, 15 μm; valve orifice, 400 μm).

sample fluid and also the dead volume is minimal. For the realization of these systems it would be much easier if two unidirectional micropumps could be replaced by one bidirectionally working micropump. We present here a way to achieve this using a special valve design and high actuation frequencies.

The dynamics of miniaturized diaphragm pumps differ very much from the dynamics of macroscopic reciprocating pumps. In previous publications [10,11] we presented an analytical model for the performance simulation of miniaturized diaphragm pumps, driven by different actuation mechanisms. The model includes the interaction between the elastic pump components and the fluidic resistance of the microvalves as well as the inertia of the fluid in the flow channels connected with the pump. This leads to a system of coupled differential equations that can be solved by the numerical simulation tool PUSI [11] or even by other system simulation tools. Within the framework of the previously presented theoretical model as well as by common sense, it does not seem to be possible to realize a bidirectional micropump with passive check valves. But the validity of the model as well as common sense are limited to actuation frequencies much lower than the resonance frequencies of the mechanical components. At higher frequencies, the resonances of the passive check valves become important. In this case we expect a phase shift between the movement of the valve and the pressure difference driving the fluid as well as the valve. In the next section we demonstrate that this effect can be used for changing the pump direction.

2. Basic principle

In Fig. 3, a miniaturized flap valve actuated by the hydrostatic pressure p_{flap} is depicted. The fluid flow through the valve depends on two parameters: (i) the displacement x of the flap defines the valve opening; (ii) the hydrostatic pressure difference p_{flap} drives the fluid through the gap of the valve opening. A detailed analysis of the flow characteristic is given in Ref. [12]. For the representation of the basic principle, we neglect the laminar pressure losses in the valve gap and thus the fluid flow can be calculated in a very simplified analysis as

$$\Phi = \mu 4lx(2p_{\text{flap}}/\rho)^{1/2} \text{ for } x \geqslant 0 \tag{1}$$

ρ corresponds to the density of the fluid and μ is an empirical geometric constant ($\mu \approx 0.5$–1.0). As a simple analogy for the transient movement of the flap, we discuss the behaviour of a driven harmonic oscillator:

$$m\ddot{x} + d\dot{x} + kx = F_{\text{flap}}(t) = Sp_{\text{flap}}(t) \tag{2}$$

The parameters m, d and k stand for the effective mass, the damping constant and the spring constant of the flap. The driving force F_{flap} can be replaced by the product of the hydrostatic pressure difference p_{flap} and the area $S = l^2$ of the valve orifice. The solution of Eq. (1) for harmonic actuation,

$$p_{\text{flap}}(t) = p^{\circ}_{\text{flap}} \exp(\mathrm{i}2\pi ft) \tag{3}$$

leads to the well-known resonance behaviour $x(f, t)$ of a damped driven oscillator:

$$x(f, t) = A(f) \exp[\mathrm{i}(2\pi ft - \alpha)] \tag{4}$$

$A(f)$ is the frequency-dependent amplitude of the valve displacement $x(f, t)$ and $\alpha(f)$ is the phase shift between the actuation pressure and the flap movement. They can be calculated from

$$A(f) = \frac{Sp^{\circ}_{\text{flap}}}{2\pi[(2\pi)^2 m^2 (f_0^2 - f^2)^2 + d^2 f^2]^{1/2}} \tag{5}$$

$$\alpha(f) = \arctan\left[\frac{fd}{2\pi m(f_0^2 - f^2)}\right] \tag{6}$$

with the resonance frequency $f_0 = (2\pi)^{-1}(k/m)^{1/2}$ of the flap in vacuum (which is much larger than the resonance frequency in the fluid environment). $A(f)$ and $\alpha(f)$ are depicted in Fig. 4(a) and (b), respectively.

In Fig. 5, the fluid flow through the microvalve is illustrated for three different driving frequencies. A harmonic pressure $p_{\text{flap}}(t)$ is assumed in all cases (Fig. 5(a)). At actuation frequencies much lower than the resonance frequency of the flap, the behaviour of the valve is quasistatic and the phase shift $\alpha(f)$ is zero. In this case the valve opening $x(t)$ (Fig. 5(b)) and the quasistatic fluid flow $\Phi(t)$ (Fig. 5(c)) through the microvalve can be calculated as

$$x(t) = kSp_{\text{flap}}(t) \tag{7}$$

$$\Phi(t) = \mu 4lkS(2p_{\text{flap}}{}^3(t)/\rho)^{1/2} \tag{8}$$

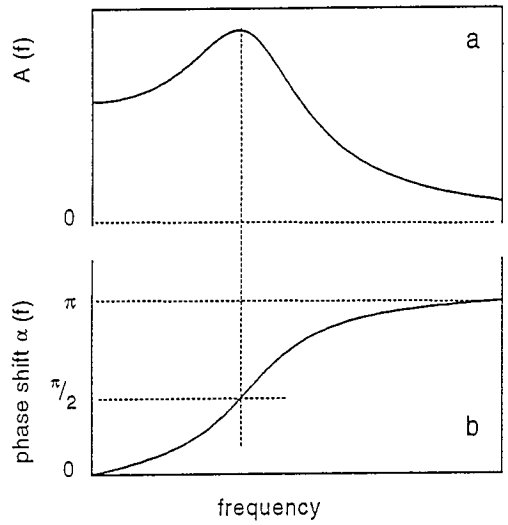

Fig. 4. Frequency-dependent amplitude (a) and phase shift (b) of a driven harmonic oscillator.

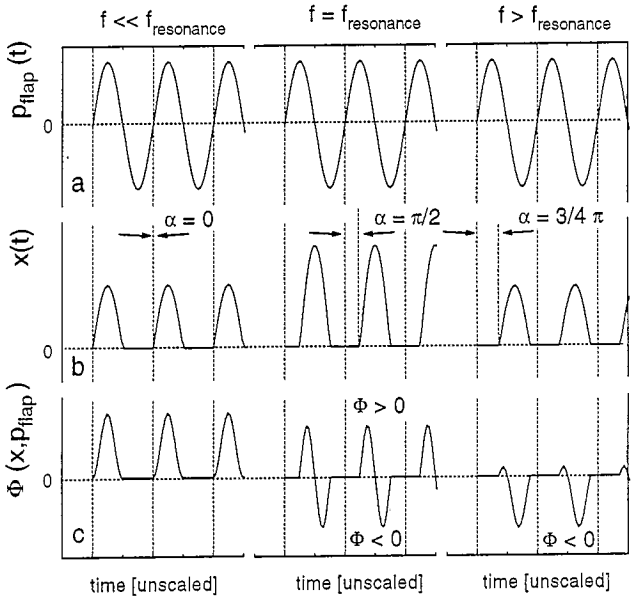

Fig. 5. Schematic interpretation of (a) transient driving pressure; (b) transient movement of the flap; and (c) transient fluid flow through the microvalve (unscaled time axis).

Only $x > 0$ is allowed for passive check valves. It can be seen that, without valve leakage, no fluid flow in the reverse direction is possible at low frequencies. As a next step, we look at an actuation frequency equal to the resonance frequency of the flap in the fluid environment. Near this frequency, the phase shift α between the driving pressure signal and the valve movement is $\pi/2$ (Fig. 5(b)). This means that the flap movement remains behind the pressure signal, which drives the fluid as well as the flap. Thus the pressure signal is partially directed to the reverse direction while the valve is still open in the forward direction. As a result of this, at half the cycle, there is a back-flow through the valve in the reverse direction which cancels out the flow in the forward direction (Fig. 5(c)). The situation becomes very interesting when the actuation frequency exceeds the resonance frequency of the valve. In this case the phase shift α is more than $\pi/2$ and the reverse flow exceeds the forward fluid flow.

It should be noticed that Fig. 5 can only be regarded as a crude qualitative approximation of the real situation inside a micropump. For instance, the effects caused by the inertia of the fluid as well as a detailed analysis of the laminar/turbulent fluid flow through the valve are not included in this example. A more detailed analysis completed by finite-element calculations is given in Ref. [12]. Furthermore, the example includes neither the interaction between two microvalves in a real pump nor an inharmonic behaviour of the transient driving pressure p_{flap}. A more appropriate theoretical description is given in Section 4.

3. Measurements

For the experiments we varied the thickness h of the flap depicted in Fig. 3 as well as the geometry of the electrostatic actuation unit (distance z between the elastic pump diaphragm and the static counter electrode; 3 μm/5 μm). In all cases the pump was driven with a supply voltage of 200 V, and the results in each run showed an excellent reproducibility. The frequency-dependent pump rate of the first group ($z = 3$ μm) is depicted in Fig. 6. For actuation frequencies between 1 and 1600 Hz the pump can be operated in its forward mode. As will be shown by detailed analysis, the frequency of zero pump rate (1600 Hz) is equal to the resonance frequency of the flap in the fluid environment [12]. This is in agreement with the mechanism discussed in Section 2. At operation frequencies between 2 and 6 kHz, the pump works in its reverse direction. The maximum pump rate in the forward direction is 250 μl min^{-1} and in the reverse direction it is 350 μl min^{-1} (for zero hydrostatic back pressure). A maximum hydrostatic back pressure of 31 000 Pa (3.1 m H_2O) has been achieved in the forward direction and 7000 Pa (0.7 m H_2O) in the reverse direction (with zero pump rate).

The thickness variation of the flap leads to a variation of the resonance frequency as well as of the fluid resistance of

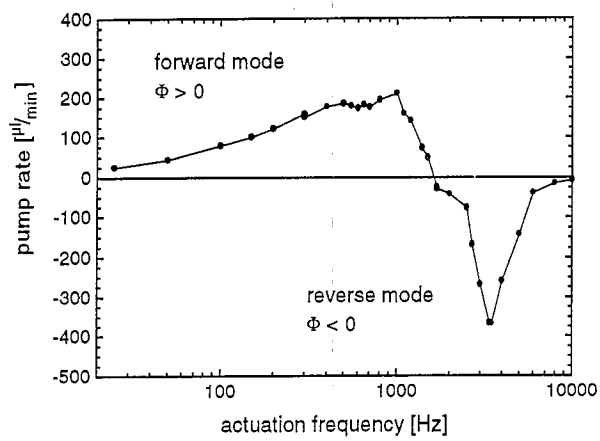

Fig. 6. Frequency-dependent pump rate without hydrostatic back pressure (layout 1: $z = 3$ μm, $h = 15$ μm).

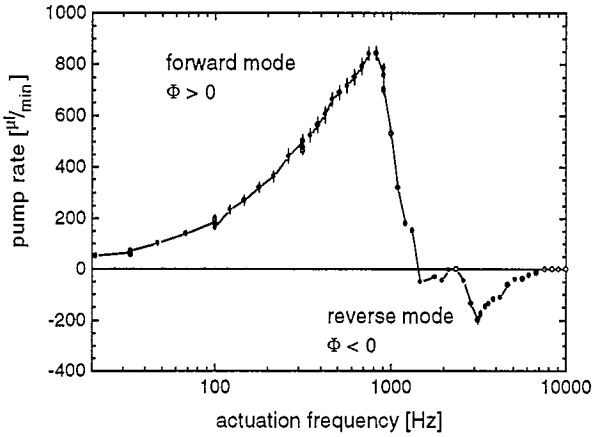

Fig. 7. Frequency-dependent pump rate without hydrostatic back pressure (layout 2: $z = 5$ µm, $h = 15$ µm).

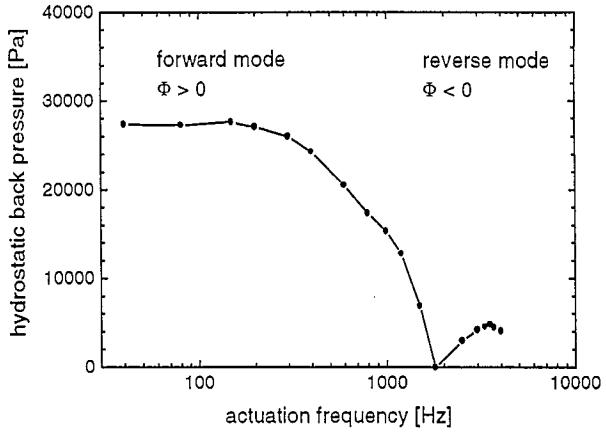

Fig. 8. Maximum hydrostatic back pressure in the forward and reverse pump modes (supply voltage, 200 V).

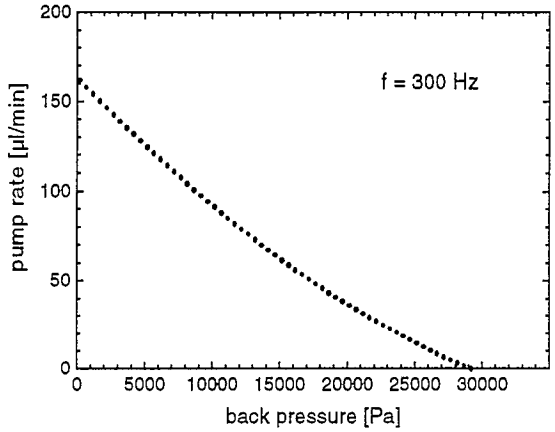

Fig. 9. Back-pressure-dependent pump rate.

the valve. For a greater thickness, the flow resistance of the valve is too large and as a consequence no fluid can be pumped at frequencies above several hundreds of hertz. At a lower thickness, the frequency-dependent pump rate is as in Fig. 6, but the frequency of zero pump rate is slightly shifted to a lower frequency. This is due to the lower resonance frequency of the flap and is in agreement with the basic principle presented above.

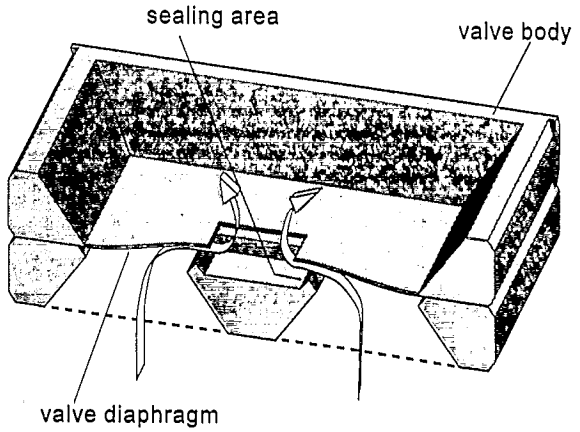

Fig. 10. Miniaturized diaphragm valve 13].

By varying the geometry of the electrostatically actuated displacement unit, the ratio between the maximum forward and reverse pump rates can be shifted (Fig. 7). We achieved maximum pump rates of 850 µl min^{-1} in the forward and 200 µl min^{-1} in the reverse direction for another set of results with a larger distance between the pump diaphragm and the counter electrode ($z = 5$ µm). The maximum hydrostatic back pressure as a function of the driving frequency is depicted in Fig. 8. It is slightly smaller compared with the first set of results given in Fig. 9. The effect is due to a small leakage of the check valves. Furthermore, we found a very interesting detail when we used two valves with different flap thicknesses. In this case, two reverse peaks can be measured in the frequency range 2–6 kHz.

In further experiments, we replaced the flap valves by diaphragm valves (Fig. 10), but we did not find a reverse pump mode. In general, the optimization of diaphragm valves as components of miniaturized pumps is more complicated than the optimization of flap valves. The reason for this is that the variation of the diaphragm thickness changes the fluidic resistance, the resonance frequency and the pressure-dependent volume displacement (fluidic capacity) of the valve as well. As has been shown in previous publications, the fluidic capacity of the valve diaphragm in the reverse direction has an unfavourable influence on the back-pressure-dependent pump performance [4,11]. This is especially important when the volume stroke of the pump is quite small (as it is in our pump, because the outer dimensions are small). In contrast to diaphragm valves, the fluidic capacity of flap valves in the reverse direction can be neglected for each design. We think that the use of diaphragm valves for bidirectional micropumps would require a general redesign of the valve layout in our case. But we do not expect any advantage compared to flap valves.

4. Theoretical pump model

As has been discussed before, the optimum pump performance in the forward as well as in the reverse direction is influenced by many parameters: the fluidic resistance and the

fluidic capacity as well as the resonance frequency of the microvalves. Furthermore, it depends on the design of the actuation unit and the geometry of the peripheral fluid system. We now sketch how the theoretical model presented up to now [10,11] can be expanded in order to include the reverse pump mode.

In the presented theory, there have been one or more (up to nine) independent pressure variables according to different steps of approximations for the dynamics of the pump [11]. In a first step, the inertia of the fluid can be neglected, leading to only one independent pressure variable, the pump chamber pressure p. By including the inertia of the movable valve part in this model, four new independent variables have to be taken into account: the displacements x_{iv5}, x_{ov} of the two valves as well as the velocities dx_{iv}/dt, dx_{ov}/dt of the valve movement. Thus the flow characteristic $\Phi_{iv}(p_{iv}, x_{iv})$ of the inlet valve depends not only on the pressure difference $p_{iv} = (p_1 - p)$ across the valve but also on the actual valve position x_{iv}. The independent variables that determine the volume displacement $V_{iv}(x_{iv})$ and $V_{ov}(x_{ov})$ of the valves are x_{iv} and x_{ov} (Fig. 11).

A procedure like that in Ref. [11] yields a system of three coupled differential equations [12]. They describe the transient behaviour of the pump chamber pressure p, as well as the valve movements x_{iv}, x_{ov}.

$$\dot{p} = \frac{\Phi_{iv} - \Phi_{ov} + \frac{dV_{iv}}{dx_{iv}}\dot{x}_{iv} - \frac{dV_{ov}}{dx_{ov}}\dot{x}_{ov} - \frac{\partial V_m}{\partial A}\bigg|_p \frac{dA}{dt}}{\frac{\partial V_m}{\partial p}\bigg|_A - \frac{dV_{gas}}{dp} + \frac{dV_o}{dp}} \tag{9}$$

$$m_{iv}\ddot{x}_{iv} + d_{iv}\dot{x}_{iv} + k_{iv}x_{iv} = S_{iv}(p_1 - p) \tag{10}$$

$$m_{ov}\ddot{x}_{ov} + d_{ov}\dot{x}_{ov} + k_{ov}x_{ov} = S_{ov}(p - p_2) \tag{11}$$

For the determination of the damping constants $d_{iv/ov}$ as well as an analytical expression for the valve flow rate, finite-element calculations were performed [12]. Ulrich et al. simulated the dynamic behaviour of a free oscillating flap in fluid surroundings in a two-dimensional model. The initial displacement of the flap is 50 μm and the transient behaviour is given in Fig. 12. The damping constant d has been extracted from Fig. 12 by fitting with

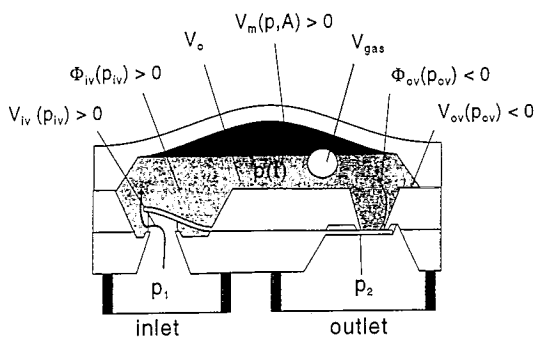

Fig. 11. Theoretical model of a miniaturized diaphragm pump including different actuation mechanisms.

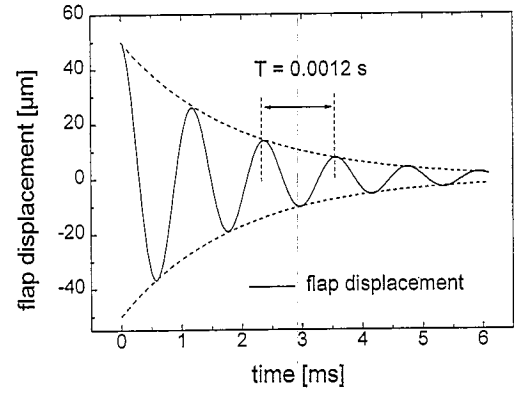

Fig. 12. Free oscillation of a flap (length, 1700 μm; thickness, 15 μm; two-dimensional model) in a water environment.

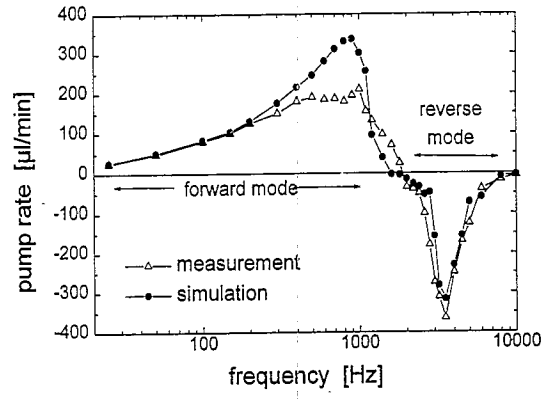

Fig. 13. Comparison between measurement and simulation of the frequency-dependent pump rate of a bidirectional micropump.

$$x(t) = A_0 \exp\left(-\frac{d}{2m}t\right)\cos(2\pi f t) \tag{12}$$

The procedure resulted in a damping constant d of 6.0×10^{-5} kg s^{-1} and in a resonance frequency of 833 Hz. These parameters, together with an analytical expression for the valve flow $\Phi(p_{iv/ov}, x_{iv/ov})$ from Ref. [12], have been used as an input to Eqs. (9)–(11). The solution in the case of an electrostatically actuated diaphragm pump results in the frequency-dependent pump rate depicted in Fig. 13. For low frequencies, we found the well-known quasistatic behaviour of miniaturized diaphragm pumps. The pump rate can be increased with a higher driving frequency. At frequencies above 1200 Hz, the flow rate decreases and becomes negative for frequencies higher than the resonance frequency of the valves. It is important to mention that the resonance frequency of the valve (1666 Hz) is twice as high as the resonance frequency of the free oscillating flap (833 Hz). The reason is the reflection of the flap at the valve seat, which doubles the frequency. In conclusion, the effect of negative flow rates can be understood due to the phase shift between the fluid movement and the flap displacement.

The agreement between measurement and simulation is quite good although the inertia of the fluid has been neglected in the derivation of Eqs. (9)–(11). In the future we shall

expand Eqs. (9)–(11) to include the inertia of the fluid, using the method demonstrated in Ref. [11].

5. Conclusions

We have presented a mechanism for changing the pump direction of miniaturized diaphragm pumps by actuation frequencies higher than the resonance frequency of the movable valve part. We suppose that the same could be achieved using other actuation mechanisms (like piezoelectric actuation) if the mechanical resonance frequency of the pump diaphragm is higher than the resonance frequency of the microvalves. In the future, bidirectional silicon micropumps will be key components of miniaturized fluid systems. The bidirectional pump mode could be used advantageously for fluid transport as well as for fluid mixing.

Acknowledgements

The authors would like to thank S. Thoma for the device fabrication and W. Geiger for the basic work on electrostatically driven micropumps.

References

[1] P. Gravesen, J. Branebjerg and O.S. Jensen, Microfluidics — a review, *Micro Mechanics Europe, Neuchâtel, Switzerland, 1993*, pp. 143–164.

[2] H.T.G. van Lintel, F.C.M. van de Pol and S. Bouwstra, A piezoelectric micropump based on micromachining of silicon, *Sensors and actuators, 15* (1988) 153–167.

[3] F.C.M. van de Pol, H.T.G. van Lintel, M. Elwenspoek and J.H.J. Fluitman, A thermopneumatic micropump based on micro-engineering techniques, *Sensors and Actuators, A21–A23* (1990) 198–202.

[4] R. Zengerle, W. Geiger, M. Richter, J. Ulrich, S. Kluge and A. Richter, Application of micro diaphragm pumps in microfluid systems, *Proc. Actuator '94, Bremen, Germany, 15–17 June, 1994*, pp. 25–29.

[5] E. Stemme and G. Stemme, A valveless diffuser/nozzle-based fluid pump, *Sensors and Actuators A, 39* (1993) 159–167.

[6] S. Shoji, S. Nakagawa and M. Esashi, Micropump and sample injector for integrated chemical analyzing systems, *Sensors and Actuators, A21–A23* (1990) 189–192.

[7] B. Büstgens, W. Bacher, W. Menz and W.K. Schomburg, Micropump manufactured by thermoplastic molding, *Proc. MEMS '94, Osio, Japan, 25–28 Feb., 1994*, pp. 18–21.

[8] T. Gerlach and H. Wurmus, Working principle and performance of the dynamic micropump, *Proc. MEMS '95, Amsterdam, Netherlands, 1995*, pp. 221–226.

[9] B.H. van de Schoot, S. Jeanneret, A. van den Berg and N.F. de Rooij, A silicon integrated miniature chemical analysis system, *Sensors and Actuators, B, 6* (1992) 57–60.

[10] R. Zengerle, M. Richter, F. Brosinger, A. Richter and H. Sandmaier, Performance simulation of microminiaturized membrane pumps, *Proc. 7th. Int. Conf. Solid-State Sensors and Actuators (Transducers '93), Yokohama, Japan, 7–10 June, 1993*, pp. 106–109.

[11] R. Zengerle and M. Richter, Simulation of microfluid systems, *J. Micromechan. Microeng., 4* (1994) 192–204.

[12] J. Ulrich, H. Füller and R. Zengerle, Static and dynamic flow simulation through a KOH-etched micro valve, *Proc. 8th Int. Conf. Solid-State Sensors and Actuators (Transducers '95), Stockholm, Sweden, 1995*, pp. 17–20.

[13] R. Zengerle, Mikro-Membranpumpen als Komponenten für Mikro-Fluidsysteme, *Ph.D. Thesis*, Verlag Shaker, Aachen, Germany, ISBN 3-8265-0216-7, 1994.